



# HHS Public Access

Author manuscript

*Am J Ophthalmol.* Author manuscript; available in PMC 2016 April 01.

Published in final edited form as:

*Am J Ophthalmol.* 2015 April ; 159(4): 634–643.e2. doi:10.1016/j.ajo.2014.12.012.

## EN FACE IMAGING OF THE CHOROID IN POLYPOIDAL CHOROIDAL VASCULOPATHY USING SWEEP-SOURCE OPTICAL COHERENCE TOMOGRAPHY

Tarek Alasil<sup>1</sup>, Daniela Ferrara<sup>1</sup>, Mehreen Adhi<sup>1</sup>, Erika Brewer<sup>1</sup>, Martin F Kraus<sup>2,3</sup>, Caroline R Bauml<sup>1</sup>, Joachim Hornegger<sup>2</sup>, James G Fujimoto<sup>3</sup>, Andre J Witkin<sup>1</sup>, Elias Reichel<sup>1</sup>, Jay S Duker<sup>1</sup>, and Nadia K Waheed<sup>1</sup>

<sup>1</sup>New England Eye Center, Tufts Medical Center, Boston, Massachusetts, USA

<sup>2</sup>Pattern Recognition Lab and School of Advanced Optical Technologies, University Erlangen Nuremberg, Erlangen, Germany

<sup>3</sup>Departments of Electrical Engineering and Computer Science and Research Laboratory of Electronics, Massachusetts Institute of Technology, Cambridge, Massachusetts, USA

### Abstract

**Objective**—To define morphological features of polypoidal choroidal vasculopathy (PCV) using en face images from swept source optical coherence tomography (SS-OCT).

**Design**—Prospective cross-sectional study.

**Methods**—Ten eyes from 6 patients with PCV and 10 eyes from 5 age-matched normal subjects. All subjects were prospectively scanned with a prototype SS-OCT system. A motion correction algorithm was applied to correct and merge scans into a single volumetric dataset. En face images were generated at intervals of 4.13  $\mu\text{m}$  (1 pixel) relative to the Bruch's membrane.

**Results**—Age  $\pm$  standard deviation for the normal group was 62.4 ( $\pm$ 12.1) years and for the PCV group was 68.3 ( $\pm$ 5.2) years. En face SS-OCT imaging of PCV eyes demonstrated the relationship between larger pigment epithelial detachments (PEDs) and small adjoining PEDs which correlated

© 2014 Elsevier Inc. All rights reserved.

Corresponding Author: Nadia K Waheed, MD, MPH, New England Eye Center, Tufts University Medical Center, 800 Washington Street, Boston, MA 02111, USA. nadiakwaheed@gmail.com.

**Financial Disclosures:** Martin F. Kraus and Joachim Hornegger receive royalties from intellectual property owned by Massachusetts Institute of Technology and licensed to Optovue Inc. James G. Fujimoto receives royalties from intellectual property owned by Massachusetts Institute of Technology and licensed to Carl Zeiss Meditech, Inc. and Optovue, Inc., and also has stock options in Optovue, Inc. Jay S. Duker is a consultant for and receives research support from Carl Zeiss Meditech, Inc.

**Contributions to Authors in each of these areas:** design of the study (T.A., D.F., J.S.D., N.K.W.); conduct of the study (T.A., D.F., M.A., E.B., M.F.K., C.B., J.H., J.G.F., A.J.W., J.S.D., N.K.W.); collection of data (T.A., M.A., E.B., C.B., A.J.W., E.R., J.S.D., N.K.W.); management (T.A., D.F., A.J.W., J.S.D., N.K.W.); analysis (T.A., D.F., M.F.K., C.B., J.H., J.G.F., A.J.W., J.S.D., N.K.W.); interpretation of the data (T.A., D.F., J.G.F., A.J.W., J.S.D., N.K.W.); preparation (T.A., D.F., M.A., E.B., A.J.W., J.S.D., N.K.W.); review (T.A., D.F., M.A., E.B., M.F.K., C.B., J.H., J.G.F., A.J.W., E.R., J.S.D., N.K.W.), and approval of the manuscript (T.A., D.F., M.A., E.B., M.F.K., C.B., J.H., J.G.F., A.J.W., E.R., J.S.D., N.K.W.).

**Publisher's Disclaimer:** This is a PDF file of an unedited manuscript that has been accepted for publication. As a service to our customers we are providing this early version of the manuscript. The manuscript will undergo copyediting, typesetting, and review of the resulting proof before it is published in its final citable form. Please note that during the production process errors may be discovered which could affect the content, and all legal disclaimers that apply to the journal pertain.

with the polypoidal lesions seen on indocyanine green angiography in all PCV eyes. En face SS-OCT demonstrated choroidal vascular abnormalities in 7 out of 7 eyes with PCV, and in 2 out of 3 enrolled fellow eyes in patients with unilateral PCV. Out of 7 PCV eyes, focal choroidal vascular dilatation was noted in 3 eyes and diffuse choroidal vascular dilatation was noted in 1 eye. In addition, a branching vascular network was noted above Bruch's membrane in 1 eye, below Bruch's membrane within the choriocapillaris in 1 eye, and in the larger choroidal vascular layer in 1 eye.

**Conclusions**—En face SS-OCT provides an *in vivo* tool to visualize the pathological features and the choroidal vasculature in PCV.

---

## Introduction

Polypoidal choroidal vasculopathy (PCV) is a term coined by Yannuzzi in 1982 [Yannuzzi LA. Idiopathic polypoidal choroidal vasculopathy: Presented at Macula Society Meeting 1982; Miami, FL, USA]. PCV is a disease characterized by multiple, recurrent serosanguineous detachments of the retinal pigment epithelium (RPE) and neurosensory retina, associated with secondary bleeding or leakage from a branching vascular network.<sup>1-4</sup> PCV likely comes in two varieties; a subset of choroidal neovascularization from a variety of causes, but most commonly due to neovascular age-related macular degeneration (AMD), or a distinct disease from AMD that is typically found in mostly darkly pigmented younger individuals, and without other fundus findings typical of AMD.

Indocyanine green angiography (ICGA) is important in securing the diagnosis of PCV, because it has the ability to demonstrate polypoidal lesions and branching vascular networks beneath the RPE that cannot be visualized using standard fluorescein angiography.<sup>5-12</sup> The use of optical coherence tomography (OCT) has become ubiquitous among retina specialists and is quite useful in the setting of PCV. The OCT features of PCV have been described and correlated with ICG findings in multiple studies.<sup>13-18</sup> A topic of interest has become the identification and characterization of polypoidal lesions and abnormal vascular networks using en face OCT images. Utilizing a spectral domain OCT-ophthalmoscope (C7; Nidek, Gamagori, Japan), investigators had reported the en face findings in PCV eyes.<sup>19, 20</sup> However, the choroid was not clearly visualized because of the signal loss beyond the RPE-Bruch's membrane complex, which is typical of SD-OCT. Swept source OCT (SS-OCT) provides long wavelength, reduced attenuation and longer imaging range when compared with SD-OCT. These properties of SS-OCT allow better penetration and improved signal strength in the choroid. Hong et al<sup>21</sup> utilized a prototype swept-source based high penetration Doppler OCT to present comprehensive visualization of the 3D structure of PCV, including feeder vessels and branching vascular networks, however the underlying anatomy of the choroidal vasculature was not analyzed in detail. Our study presents the en face imaging features of the retina and choroid in PCV patients using a prototype 1050 nm wavelength SS-OCT instrument.

## Methods

We prospectively enrolled patients with PCV at the New England Eye Center at Tufts Medical Center between December 2013 and May 2014, and age-matched healthy

volunteers. Study protocols were approved by the Institutional Review Board of Tufts Medical Center and Massachusetts Institute of Technology and were in accordance with the Health Insurance Portability and Accountability Act. The research adhered to the tenets of the Declaration of Helsinki for research involving human subjects.

Signed informed consent was obtained prior to SS-OCT image acquisition. Subjects were examined with a prototype SS-OCT system operating at 1050 nm for enhanced choroidal penetration. The details of this prototype machine have been previously reported and validated.<sup>22, 23</sup> Briefly, the system employs a commercially-available 100 kHz wavelength-swept semiconductor laser (Axsun Technologies Inc., Billerica, MA) with a sweep bandwidth of ~100 nm, providing a tissue axial resolution of 6  $\mu\text{m}$ . The light incident on the eye was 1.9 mW, which is consistent with the American National Standard Institute (ANSI) standards for safe ocular exposure. Three dimensional 6 $\times$ 6 mm scans with 400 $\times$ 400 axial scans or 12 $\times$ 12 mm scans with 500 $\times$ 500 axial scans were obtained, each acquired within 1.7 seconds. For each subject, at least two orthogonal volumetric scans were acquired, processed with software for motion correction, and merged into a single volumetric dataset to enhance the signal.<sup>24</sup>

A semi-automatic algorithm with manual correction capabilities was developed and was utilized to flatten the scans using Bruch's membrane as a reference, in order to generate a reference surface for en face display. En face images through the retina, RPE, and choroid were extracted at varying depths every 4.13  $\mu\text{m}$  (1 pixel, corresponding to the digital resolution of OCT images) using Bruch's membrane as a reference surface. Image J Software (National Institutes of Health, Bethesda, MD; available at <http://rsb.info.nih.gov/ij/index.html>) was used to facilitate an en face image view in an orthogonal three-dimensional fashion, where B-scans and C-scans could be precisely correlated.

Using en face SS-OCT imaging, the transition from the fine homogeneous choriocapillaris (CC) into the choroidal vascular layer (CV), where the choroidal vessels became distinct was apparent. The most representative C-scan for the transition between CC and CV layers was identified. Using this, an estimate of the CC thickness was performed by counting the number of axial pixels between RPE and the transition zone and then multiplying by the pixel dimension (4.13  $\mu\text{m}$ ). The lumen of the choroidal vessels started to enlarge from the transition zone going through the inner choroid towards the outer choroid. The choroidal-scleral interface was easily identified on en face display by displacement of the choroidal vasculature with the white sclera. Similarly, the CV thickness was calculated by counting the axial pixels in between the transition zone and the choroidal-scleral interface and performing the above-mentioned calculation. Subsequently, the total choroidal thickness was calculated by adding the CC and CV thicknesses.

Morphological features of PCV were identified by 2 independent authors (TA and DF) using a standard protocol to analyze color photographs, fundus autofluorescence, fluorescein angiography, ICGA, and SS-OCT images. Disagreement between the 2 observers was resolved by open adjudication.

## Results

Ten eyes from 6 Asian patients with PCV and 10 eyes from 5 age-matched normal subjects (1 Asian and 4 Caucasians) were enrolled in a prospective cross-sectional study. Age  $\pm$  standard deviation was  $68.3 \pm 5.2$  years in the PCV group and  $62.4 \pm 12.1$  years in the normal group. Visual acuity ranged between 20/30 and 20/200 in the PCV group, and was 20/30 or better in the normal group. One PCV patient had history of enucleation of the contralateral eye because of massive hemorrhage. One patient with unilateral peripheral PCV lesion refused to have the fellow eye scanned. Five PCV eyes had received no treatment and two eyes underwent intravitreal injections with anti-vascular endothelial growth factor agent in the past. ICGA identified polypoidal lesions in all 7 PCV eyes. The fellow eyes in 3 patients with unilateral PCV were scanned with SS-OCT as well. Table 1 further demonstrates the demographics of patients with PCV.

### Qualitative Analysis

En face SS-OCT imaging allowed virtual sectioning of the pathological area of interest in consecutive scans through the retina, RPE, and choroid. One or more dome-shaped pigment epithelial detachments (PEDs) were visualized on SS-OCT cross-sectional scans in all 7 PCV eyes. On en face SS-OCT scans anterior to Bruch's membrane, PEDs were visualized as a highly reflective oval or circular line of RPE, which corresponded to the outline of the PED. Irregularities in the outline of larger PEDs were identified as small adjoining PEDs, and correlated with polypoidal lesions seen on ICGA in all 7 PCV eyes (Figures 1, 2, 3, 4 and 5). The material within the smaller PEDs representing polypoidal lesions was typically more highly reflective than the material in the larger adjoining PED (Figure 1).

Cross-sectional SS-OCT imaging demonstrated the "double layer sign" adjoining more highly elevated PEDs and polyps in 5 out of 7 PCV eyes (Figures 1, 4, and 5). The "double layer sign" was identified in previous studies as two hyperreflective lines representing the RPE and Bruch's membrane, where an abnormal vascular network resides.<sup>13, 14</sup> Fibrotic PEDs indicating chronicity were identified in 2 out of 7 PCV eyes (Figures 4 and 5). The feeder vessel was visualized in 3 out of 7 PCV eyes as a thin hyporeflective band that started in the choroid and penetrated Bruch's membrane to reach the small PED where the polypoidal lesion was situated (Figures 5 and 6).

En face SS-OCT demonstrated choroidal vascular abnormalities in 7 out of 7 eyes with PCV, and in 2 out of 3 enrolled fellow eyes in patients with unilateral PCV. Out of seven PCV eyes, focal choroidal vascular dilatation was noted in 3 eyes while diffuse choroidal vascular dilatation was noted in 1 eye. In addition, a branching vascular network was noted above Bruch's membrane in 1 eye, below Bruch's membrane (within the choriocapillaris) in 1 eye, and in the deeper choroidal vascular layer in 1 eye. The branching vascular networks above and below Bruch's membrane correlated with the double layer sign seen on cross-sectional scans (Figures 1 and 3). Out of three fellow eyes that were examined in patients with unilateral PCV, focal choroidal vascular dilatation was noted in 1 eye (Figure 7), diffuse choroidal vascular dilatation was noted in 1 eye, and no obvious choroidal vascular abnormalities were noted in 1 eye.

## Quantitative Analysis

The CC, CV, and total choroid mean thicknesses (around the area of pathology) in PCV eyes were 41.3  $\mu\text{m}$ , 274.0  $\mu\text{m}$ , and 315.3  $\mu\text{m}$ , respectively. The subject with superior peripheral PCV lesion was excluded from the comparison, since the choroidal thickness measurements were taken around the peripheral PCV lesion. The CC, CV, and total choroidal mean thickness in the fellow eyes were 42.7  $\mu\text{m}$ , 293.2  $\mu\text{m}$ , and 335.9  $\mu\text{m}$ , respectively. The fellow eye choroidal thickness measurements were not significantly different from the PCV affected eyes, and the *p-values* for CC, CV, and total choroidal thicknesses were, respectively, 0.64, 0.74, and 0.73. Table 2 further demonstrates these measurements.

When compared to the normal eyes, the PCV eyes demonstrated significantly thinner CC (*p-value*= 0.03). However, the CV and total choroidal thicknesses were not significantly different between PCV and normal eyes (*p-values* were 0.7 and 0.99, respectively). Table 3 further delineates these results.

## Discussion

Polypoidal choroidal vasculopathy (PCV) is characterized by polypoidal neovascular lesions connected to a branching vascular network.<sup>3,6-9, 25-28</sup> Investigators proposed problems with the auto-regulation of blood flow within the choroid as a predisposing factor which may lead to development of PCV. Polypoidal lesions are thought to form because of a localized delay in choroidal capillary lobular filling, causing capillary and venous congestion in the affected lobules. The impaired choroidal circulation results in the formation of the polypoidal lesions, and impaired function of the RPE-Bruch's membrane complex produces a PED.<sup>28, 29</sup> The presence of large serosanguineous PEDs in eyes with PCV has been established as a typical presentation, due to the propensity for polyps to bleed between the RPE and Bruch's membrane.<sup>6-10, 25, 30</sup>

Using en face SS-OCT, the relationship between polypoidal lesions and adjacent PEDs can be more clearly demonstrated. A protrusion from the wall of the PED often corresponds with the polypoidal lesions seen on ICGA; these lesions contain more highly reflective material on OCT compared to the adjacent serous PED, when present. Our results are in agreement with previous OCT studies examining PCV.<sup>19, 20</sup>

Histological studies have examined surgical specimens obtained from PCV eyes to better understand and locate the polypoidal lesions and the feeding branching vascular networks. Although dilated choroidal vessels were observed beneath Bruch's membrane by Okubo<sup>31</sup> and MacCumber<sup>32</sup>, many other histologic studies found fibrovascular tissues within or above Bruch's membrane.<sup>32-37</sup> Our cross-sectional SS-OCT scans revealed mild elevations of the RPE, associated with a second underlying highly reflective line, forming a "double-layer" sign in 5 out of 7 PCV eyes, which was previously reported as a typical feature of the branching vascular network in PCV.<sup>12,13,38</sup> Our en face SS-OCT findings suggested that branching vascular networks in PCV can be seen either above Bruch's membrane or below Bruch's membrane (within the choriocapillaris or larger choroidal vascular layers). Furthermore, a group of dilated choroidal vessels (focal or diffuse) were noted, at variable depths, within the choroidal vascular layer below the pathological area.

The choriocapillaris is difficult to visualize using standard SD-OCT scanning protocols, and direct visualization of CC requires angiography.<sup>39</sup> However, using en face SS-OCT imaging, we were able to see the transition from the fine homogeneous CC into the choroidal vascular zone, where the choroidal vessels became distinct and increased in size moving away from the CC.

Examining the fellow eyes in 3 patients with unilateral PCV in our cohort revealed choroidal vascular dilatation in 2 out of 3 eyes. One of the PCV patients in our cohort had bilateral PCV and another patient had her fellow eye enucleated after a massive retinal hemorrhage. These findings suggest that abnormalities of the choroidal vasculature may precede the development of PCV, and that PCV is likely often a bilateral disease with unilateral presentation. Future en face OCT studies with a larger number of PCV patients are warranted to further investigate this finding, especially since PCV involvement was reported to be mostly unilateral (90% of patients) in a large Japanese cohort of 100 patients with PCV.<sup>10</sup> En face SS-OCT may provide a useful tool to screen the choroid of unaffected eyes in patients with unilateral PCV.

Our study has a number of limitations. First, our sample size is relatively small compared to the Japanese studies. However, PCV has been reported to be more common in Asians when compared to Caucasians.<sup>10</sup> Studies have shown that one fourth to one half of the elderly patients with neovascular age-related macular degeneration in Japan was diagnosed with PCV.<sup>10,11</sup> Second, the cross-sectional nature of our study prevents us from drawing conclusions about the progression of pathological features in PCV. Third, the interpretation of en face SS-OCT images can be challenging, as they are not the standard images clinicians are used to evaluate. Complex software must be used for motion correction as well as flattening of B-scan images in order to generate a reference surface for en face display. When imaging the choroid, shadowing from large PEDs (Figure 1) and retinal exudates (Figure 5) can obscure details of the choroid, sometimes making the images difficult to interpret. Despite these limitations, we were able to visualize the relationship between polypoidal lesions, PEDs, and branching vascular networks, as well as underlying abnormalities of the choroidal vessels in eyes with PCV, using a prototype SS-OCT system with long wavelength, three-dimensional motion correction algorithms and the application of enface displays. In future studies, the improved SS-OCT image acquisition speed will facilitate the development of optical coherence angiography, which will deliver noninvasive mapping of the retinal and choroidal vasculature, provide new insights into the pathophysiology of PCV, and may ultimately guide the development of new treatment strategies.

In conclusion, using en face SS-OCT imaging, we describe the visualization of polypoidal structures underneath the RPE and above Bruch's membrane, branching vascular networks above and below Bruch's membrane, and underlying choroidal vascular abnormalities in eyes with PCV. In addition, choroidal vascular abnormalities may be seen in fellow eyes of PCV. Therefore, en face SS-OCT may provide an *in vivo* tool to better understand the pathophysiology of PCV.

## Acknowledgments

*Funding/Support:* National Institute of Health (R01-EY011289-28, R01-EY013178-12, R01-CA075289-16), Air Force Office of Scientific Research (FA9550-10-1-0551 and FA9550-12-1-0499), An Unrestricted Grant from Research to Prevent Blindness to the New England Eye Center, Tufts University School of Medicine, Massachusetts Lions Clubs, Deutsche Forschungsgemeinschaft (DFG-HO-1791/11-1, DFG Training Group 1773, DFG-GSC80-SAOT). The sponsors had no role in the design or conduct of this research.

None

## References

1. Stern RM, Zakov ZN, Zegarra H, Gutman FA. Multiple recurrent serosanguineous retinal pigment epithelial detachments in black women. *Am J Ophthalmol.* 1985; 100(4):560–69. [PubMed: 2413762]
2. Gass, JDM. *Stereoscopic Atlas of Macular Diseases: Diagnosis and Treatment.* Vol. 1. St Louis, Mo: CV Mosby; 1987. p. 200
3. Yannuzzi LA, Sorenson J, Spaide RF, Lipson B. Idiopathic polypoidal choroidal vasculopathy (IPCV). *Retina.* 1990; 10(1):1–8. [PubMed: 1693009]
4. Kleiner RC, Brucker AJ, Johnson RL. The posterior uveal bleeding syndrome. *Retina.* 1990; 10(1): 9–17. [PubMed: 2343198]
5. Perkovich BT, Zakov ZN, Berlin LA, Weidenthal D, Avins LR. An update on multiple recurrent serosanguineous retinal pigment epithelial detachments in black women. *Retina.* 1990; 10(1):18–26. [PubMed: 2188313]
6. Spaide RF, Yannuzzi LA, Slakter JS, Sorenson J, Orlach DA. Indocyanine green videoangiography of idiopathic polypoidal choroidal vasculopathy. *Retina.* 1995; 15(2):100–10. [PubMed: 7542796]
7. Yannuzzi LA, Ciardella A, Spaide RF, Rabb M, Freund KB, Orlock DA. The expanding clinical spectrum of idiopathic polypoidal choroidal vasculopathy. *Arch Ophthalmol.* 1997; 115(4):478–85. [PubMed: 9109756]
8. Yannuzzi LA, Wong DW, Sforzolini BS, et al. Polypoidal choroidal vasculopathy and neovascularized age-related macular degeneration. *Arch Ophthalmol.* 1999; 117(11):1503–10. [PubMed: 10565519]
9. Uyama M, Matsubara T, Fukushima I, et al. Idiopathic polypoidal choroidal vasculopathy in Japanese patients. *Arch Ophthalmol.* 1999; 117(8):1035–42. [PubMed: 10448746]
10. Sho K, Takahashi K, Yamada H, et al. Polypoidal choroidal vasculopathy: incidence, demographic features, and clinical characteristics. *Arch Ophthalmol.* 2003; 121(10):1392–6. [PubMed: 14557174]
11. Maruko I, Iida T, Saito M, et al. Clinical characteristics of exudative age-related macular degeneration in Japanese patients. *Am J Ophthalmol.* 2007; 144(1):15–22. [PubMed: 17509509]
12. Tsujikawa A, Sasahara M, Otani A, et al. Pigment epithelial detachment in polypoidal choroidal vasculopathy. *Am J Ophthalmol.* 2007; 143(1):102–11. [PubMed: 17101112]
13. Kim JH, Kang SW, Kim TH, Kim SJ, Ahn J. Structure of polypoidal choroidal vasculopathy studied by colocalization between tomographic and angiographic lesions. *Am J Ophthalmol.* 2013; 156(5):974–80. [PubMed: 23958701]
14. Park SY, Kim SM, Song YM, Sung J, Ham DI. Retinal thickness and volume measured with enhanced depth imaging optical coherence tomography. *Am J Ophthalmol.* 2013; 156(3):557–66. [PubMed: 23769194]
15. Ueno C, Gomi F, Sawa M, Nishida K. Correlation of indocyanine green angiography and optical coherence tomography findings after intravitreal ranibizumab for polypoidal choroidal vasculopathy. *Retina.* 2012; 32(10):2006–13. [PubMed: 22772392]
16. Coscas F, Coscas G, Souied E. Polypoidal choroidal vasculopathy and macroaneurysm: respective roles of scanning laser ophthalmoscopy. *Eur J Ophthalmol.* 2011; 21(3):331–5. [PubMed: 20853255]

17. Ojima Y, Hangai M, Sakamoto A, et al. Improved visualization of polypoidal choroidal vasculopathy lesions using spectral-domain optical coherence tomography. *Retina*. 2009; 29(1): 52–9. [PubMed: 18827738]
18. Rosen RB, Hathaway M, Rogers J, et al. Simultaneous OCT/SLO/ICG imaging. *Invest Ophthalmol Vis Sci*. 2009; 50(2):851–60. [PubMed: 18952928]
19. Kameda T, Tsujikawa A, Otani A, et al. Polypoidal choroidal vasculopathy examined with en face optical coherence tomography. *Clin Experiment Ophthalmol*. 2007; 35(7):596–601. [PubMed: 17894678]
20. Saito M, Iida T, Nagayama D. Cross-sectional and en face optical coherence tomographic features of polypoidal choroidal vasculopathy. *Retina*. 2008; 28(3):459–64. [PubMed: 18327139]
21. Hong YJ, Miura M, Makita S, et al. Noninvasive investigation of deep vascular pathologies of exudative macular diseases by high-penetration optical coherence angiography. *Invest Ophthalmol Vis Sci*. 2013; 54(5):3621–31. [PubMed: 23633664]
22. Potsaid B, Baumann B, Huang D, et al. Ultrahigh speed 1050nm swept source /Fourier domain OCT retinal and anterior segment imaging at 100,000 to 400,000 axial scans per second. *Opt Exp*. 2010; 18(19):20029–48.
23. Ferrara D, Mohler KJ, Waheed N, et al. Enface enhanced-depth swept-source optical coherence tomography features of chronic central serous chorioretinopathy. *Ophthalmology*. 2014; 121(3): 719–26. [PubMed: 24289918]
24. Kraus MF, Potsaid B, Mayer MA, et al. Motion correction in optical coherence tomography volumes on a per A-scan basis using orthogonal scan patterns. *Biomed Opt Express*. 2012; 3(6): 1182–99. [PubMed: 22741067]
25. Uyama M, Wada M, Nagai Y, et al. Polypoidal choroidal vasculopathy: natural history. *Am J Ophthalmol*. 2002; 133(5):639–48. [PubMed: 11992861]
26. Yuzawa M, Mori R, Kawamura A. The origins of polypoidal choroidal vasculopathy. *Br J Ophthalmol*. 2005; 89(5):602–7. [PubMed: 15834093]
27. Moorthy RS, Lyon AT, Rabb MF, Spaide RF, Yannuzzi LA, Jampol LM. Idiopathic polypoidal choroidal vasculopathy of the macula. *Ophthalmology*. 1998; 105(8):1380–5. [PubMed: 9709746]
28. Costa RA, Navajas EV, Farah ME, Calucci D, Cardillo JA, Scott IU. Polypoidal choroidal vasculopathy: angiographic characterization of the network vascular elements and a new treatment paradigm. *Prog Retin Eye Res*. 2005; 24(5):560–86. [PubMed: 16005406]
29. Yanoff, M.; Duker, JS. *Ophthalmology*. Third Edition. St Louis, Mo: Mosby Elsevier; 2009.
30. Ahuja RM, Stanga PE, Vingerling JR, Reck AC, Bird AC. Polypoidal choroidal vasculopathy in exudative and haemorrhagic pigment epithelial detachments. *Br J Ophthalmol*. 2000; 84(5):479–84. [PubMed: 10781511]
31. Okubo A, Sameshima M, Uemura A, Kanda S, Ohba N. Clinicopathological correlation of polypoidal choroidal vasculopathy revealed by ultrastructural study. *Br J Ophthalmol*. 2002; 86(10):1093–8. [PubMed: 12234885]
32. MacCumber MW, Dastgheib K, Bressler NM, et al. Clinicopathologic correlation of the multiple recurrent serosanguineous retinal pigment epithelial detachments syndrome. *Retina*. 1994; 14(2): 143–52. [PubMed: 8036324]
33. Spraul CW, Grossniklaus HE, Lang GK. Idiopathic polypoid choroid vasculopathy. *Klin Monatsbl Augenheilkd*. 1997; 210(6):405–6. [PubMed: 9333671]
34. Lafaut BA, Aisenbrey S, Van den Broecke C, Bartz-Schmidt KU, Heimann K. Polypoidal choroidal vasculopathy pattern in age-related macular degeneration: a clinicopathologic correlation. *Retina*. 2000; 20(6):650–4. [PubMed: 11131419]
35. Rosa RH Jr, Davis JL, Eifrig CW. Clinicopathologic reports, case reports, and small case series: clinicopathologic correlation of idiopathic polypoidal choroidal vasculopathy. *Arch Ophthalmol*. 2002; 120(4):502–8. [PubMed: 11934327]
36. Terasaki H, Miyake Y, Suzuki T, Nakamura M, Nagasaka T. Polypoidal choroidal vasculopathy treated with macular translocation: clinical pathological correlation. *Br J Ophthalmol*. 2002; 86(3): 321–7. [PubMed: 11864892]



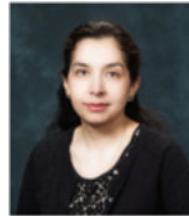
37. Kuroiwa S, Tateiwa H, Hisatomi T, Ishibashi T, Yoshimura N. Pathological features of surgically excised polypoidal choroidal vasculopathy membranes. *Clin Experiment Ophthalmol.* 2004; 32(3): 297–302. [PubMed: 15180844]
38. Sato T, Kishi S, Watanabe G, Matsumoto H, Mukai R. Tomographic features of branching vascular networks in polypoidal choroidal vasculopathy. *Retina.* 2007; 27(5):589–94. [PubMed: 17558321]
39. Choi W, Mohler KJ, Potsaid B, et al. Choriocapillaris and Choroidal Microvasculature Imaging with Ultrahigh Speed OCT Angiography. *PLoS One.* 2013; 8(12):e81499. [PubMed: 24349078]

## Biographies



### **Tarek Alasil, MD**

Tarek Alasil, MD did research for this paper during his optical coherence tomography research fellowship at the New England Eye Center and Tufts University School of Medicine in Boston, MA. He is currently a resident at the Department of Ophthalmology and Visual Sciences at Yale University School of Medicine. His main research interests focus on ophthalmic imaging with optical coherence tomography. He has published over 20 original articles, major reviews, case reports, and book reviews.



### **Nadia K Waheed, MD, MPH**

Dr. Waheed is an Assistant Professor of Ophthalmology at the Tufts University School of Medicine in Boston. She received her medical degree *summa cum laude* from the Aga Khan University Medical School and a Master degree from the Harvard School of Public Health. She completed a residency in Ophthalmology and a Fellowship in Retina at the Massachusetts Eye and Ear Infirmary. Her research interests include ocular imaging, diabetic eye disease and age related macular degeneration.

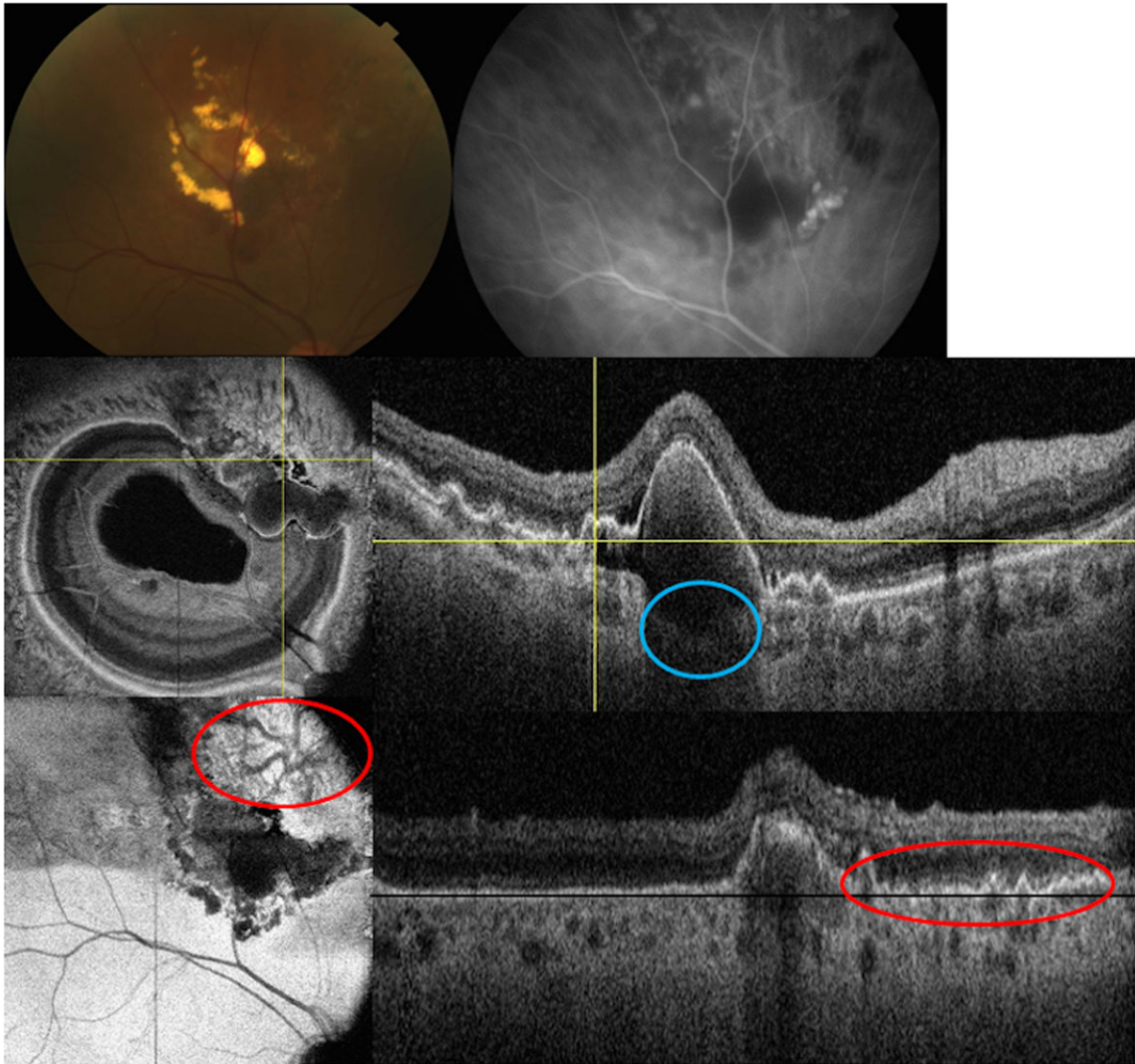


**Figure 1.**

Multimodal imaging of the right eye of a 63-year-old Asian woman with polypoidal choroidal vasculopathy (peripheral to the macula). (Top left) color picture (Top right) late-phase indocyanine green angiography (ICGA) are shown (Middle left) en face swept source optical coherence tomography (SS-OCT) is showing the pigment epithelial detachment (PED) with protrusion where the polyp is located (crossing yellow lines) (Middle right) corresponding B-scan; there is a shadow artifact from the large PED which obscures the details of the choroid underneath (blue circle) (Lower left) flattened en face SS-OCT revealed dilated choroidal vascular network below retinal pigment epithelium and above Bruch's membrane (red circle) (Lower right) corresponding flattened B-scan (black line represents the C-scan level).

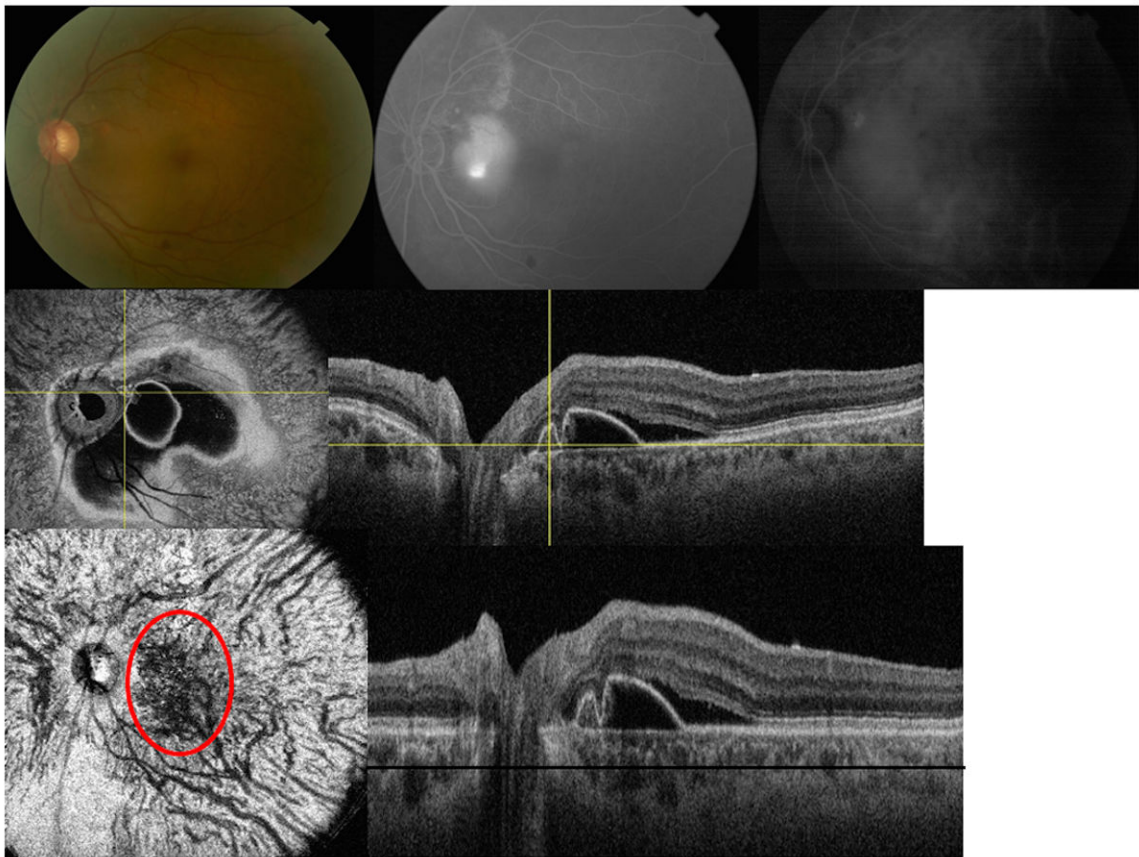


**Figure 2.** Multimodal imaging of the left eye of a 61-year-old Asian woman with polypoidal choroidal vasculopathy (peripapillary lesion). (Top left) fundus photo is showing the peripapillary lesion (Top middle) fluorescein angiogram (Top right) indocyanine green angiography (ICGA) is showing the polypoidal lesion and corresponding abnormal choroidal vascular network (Middle left) en face swept source optical coherence tomography (SS-OCT) is showing the pigment epithelial detachment with protrusion where the polyp is located and easily visualized (crossing yellow lines) (Middle right) corresponding B-scan (Lower left) flattened en face SS-OCT of the choroid is showing abnormal choroidal vascular network within the choroidal vascular layer (red circle) (Lower right) corresponding flattened B-scan (black line represents the C-scan level).

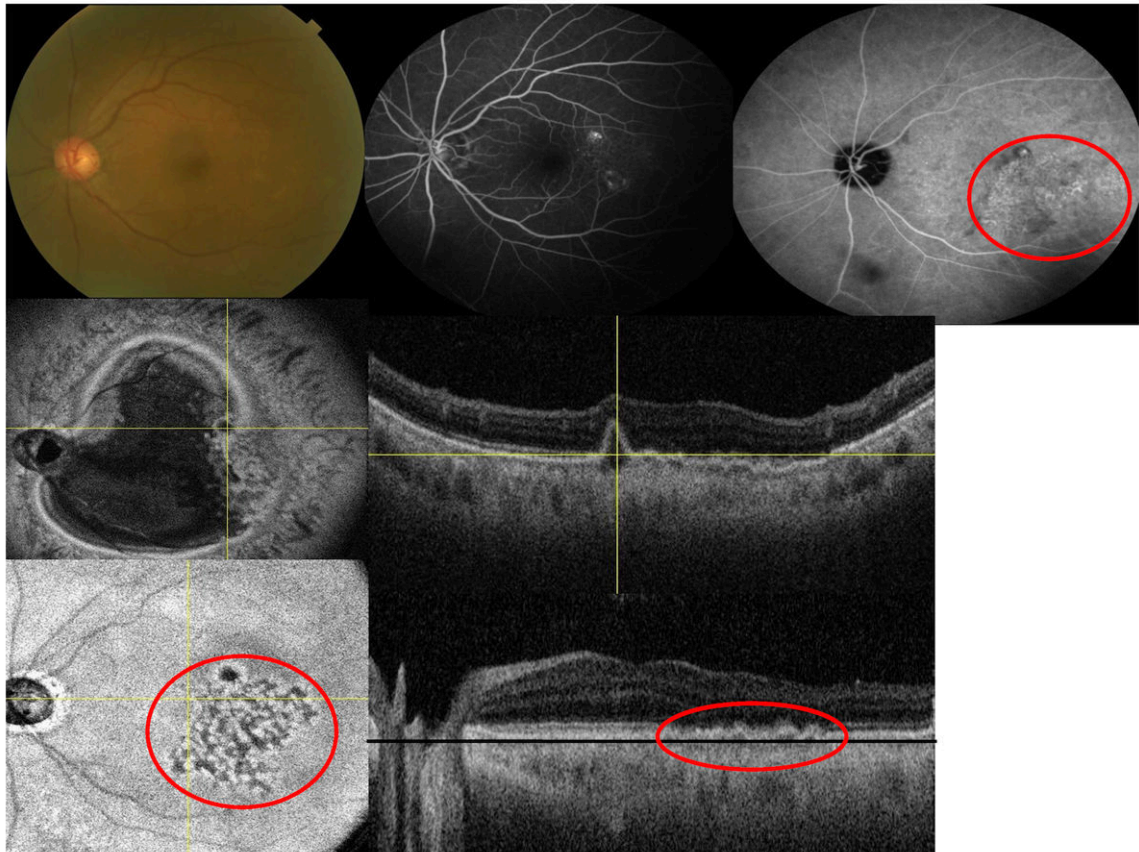


**Figure 3.** Multimodal imaging of the left eye of a 74-year-old Asian woman with polypoidal choroidal vasculopathy (juxtafoveal lesion). (Top left) fundus picture (Top middle) fluorescein angiogram (Top right) indocyanine green angiography (ICGA) (Middle left) en face swept source optical coherence tomography (SS-OCT) is showing the pigment epithelial detachment with adjacent abnormal vascular network (red circle) (Middle right) corresponding B-scan is showing the branching vascular network (Lower left) flattened en face SS-OCT of the choroid is showing abnormal choroidal vascular network within the choriocapillaris layer just beneath the Bruch's membrane (red circle) (Lower right) corresponding flattened B-scan (the black line represent the C-scan level just beneath the Bruch's membrane).

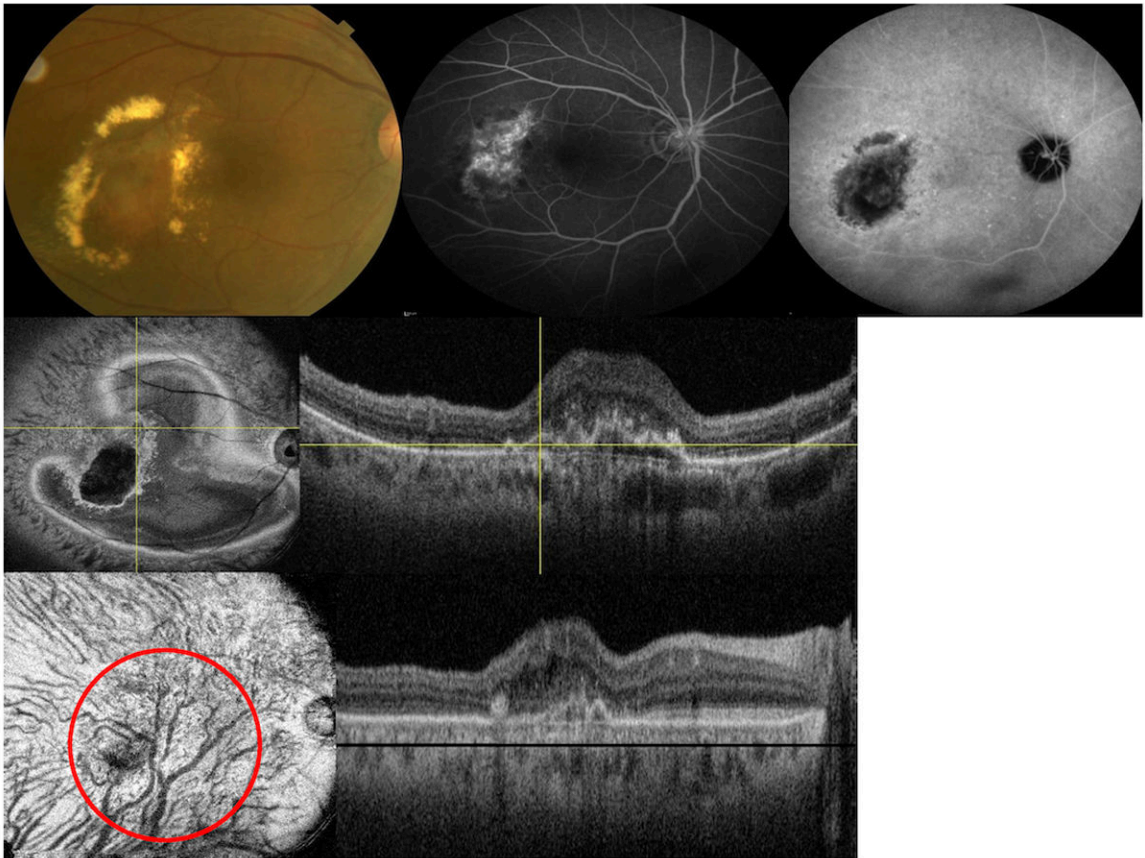


**Figure 4.**

Multimodal imaging of the right eye of a 74-year-old Asian woman with polypoidal choroidal vasculopathy (juxtafoveal lesion). (Top left) fundus picture is showing an area of a polyp and surrounding hard exudates (Top middle) fluorescein angiogram (Top right) late-phase indocyanine green angiography (ICGA) (Middle left) en face swept source optical coherence tomography (SS-OCT) is showing the pigment epithelial detachment with adjacent abnormal vascular network (Middle right) corresponding B-scan is showing the double layer sign (Lower left) flattened en face SS-OCT image is showing abnormal choroidal vascular dilatation within the choroidal vascular layer (red circle) (Lower right) corresponding flattened B-scan (black line is showing the C-scan level).

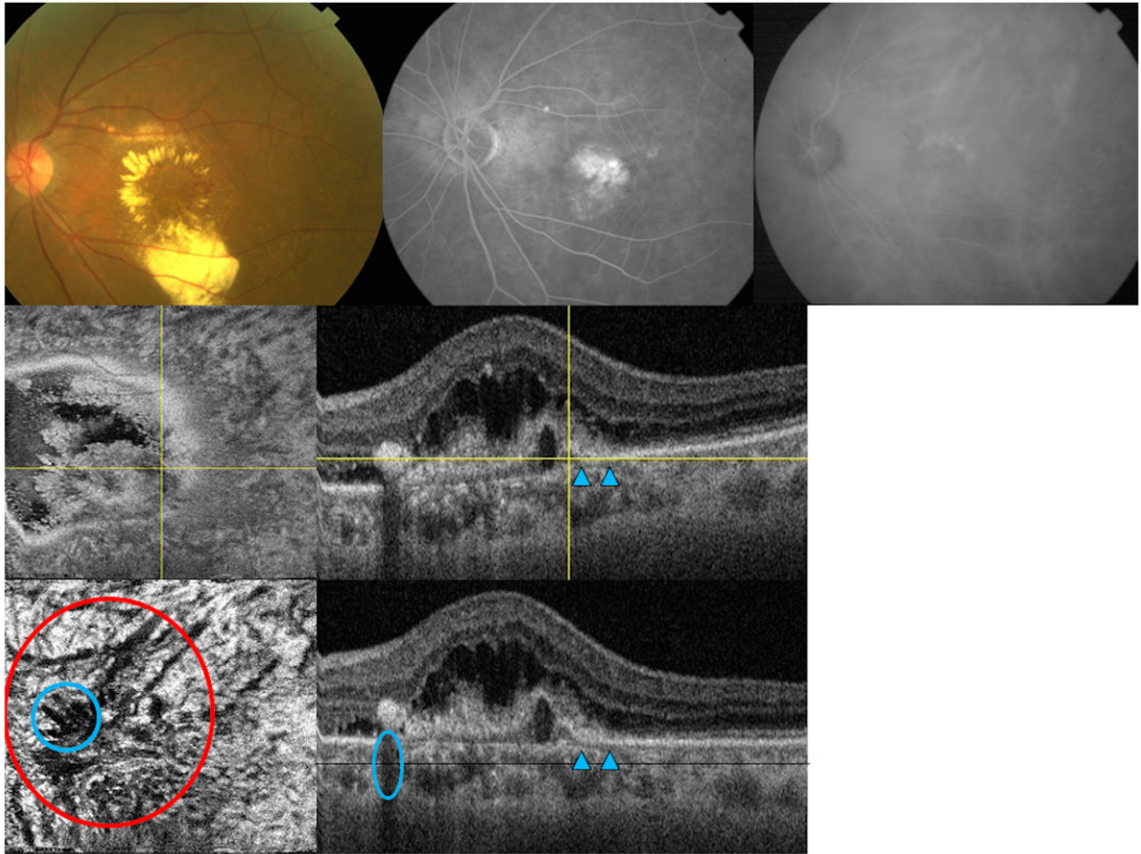


**Figure 5.**

Multimodal imaging of the left eye of a 69-year-old Asian woman with polypoidal choroidal vasculopathy (subfoveal lesion). (Top left) fundus picture is showing an area of a polyp and surrounding exudates (Top middle) fluorescein angiogram (Top right) late phase indocyanine green angiography (ICGA) are shown (Middle left) en face swept source optical coherence tomography (SS-OCT) image is showing the fibrovascular component above Bruch's membrane (Middle right) corresponding B-scan is showing the feeder vessel as hyporeflective line (arrowheads) penetrating through the Bruch's membrane to feed the polyp (yellow crossing lines) (Lower left) flattened en face SS-OCT image is showing choroidal vascular dilatation in the choroidal vascular layer (red circle), shadow artifacts from the retina exudates are marked with a blue circle (Lower right) corresponding flattened B-scan is showing the fibrovascular structures and feeder vessel (arrowheads).

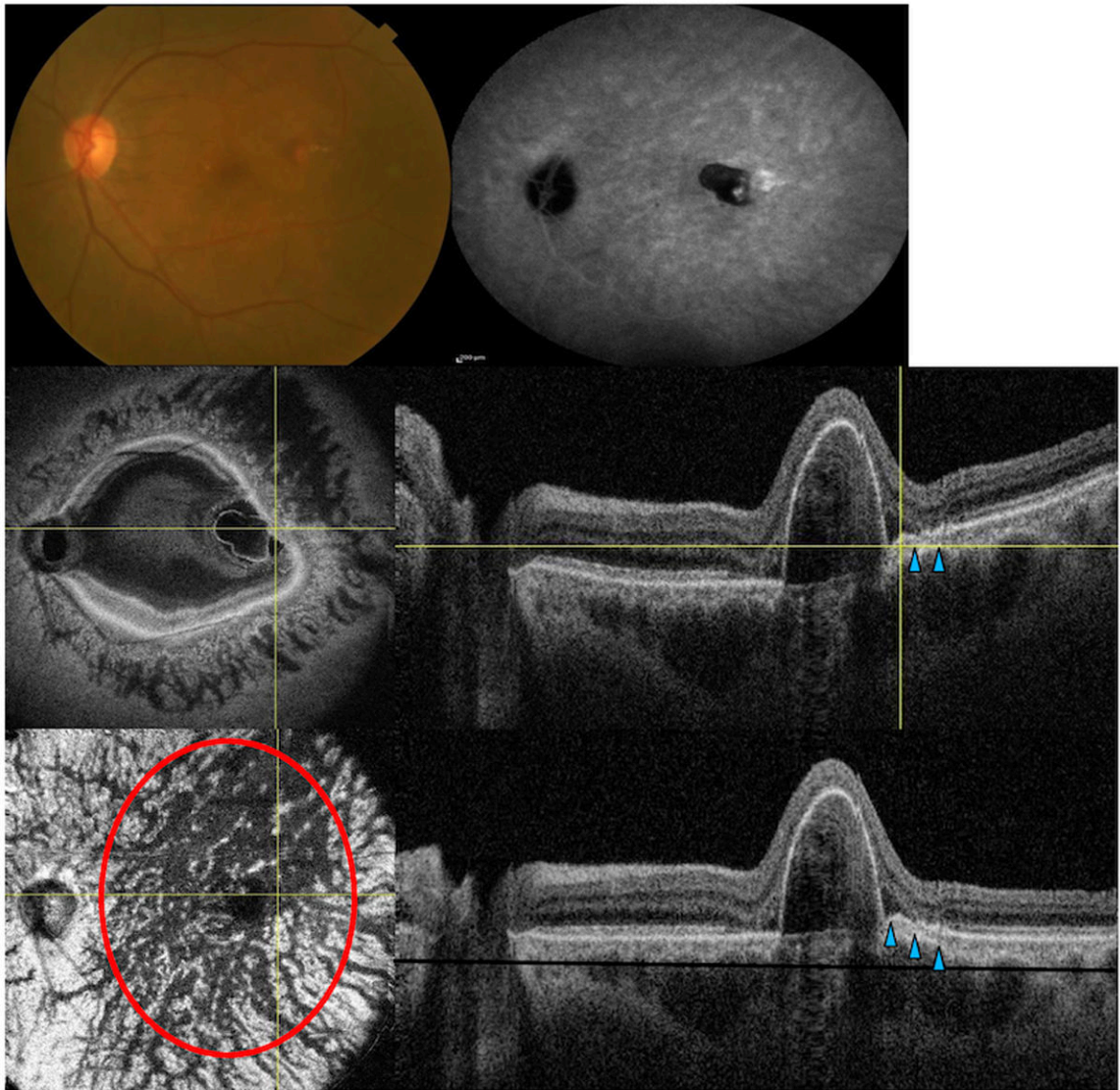


**Figure 6.** Multimodal imaging of the left eye of a 71-year-old Asian woman with polypoidal choroidal vasculopathy (extrafoveal lesion). (Top left) fundus picture (Top right) late phase indocyanine green angiography (ICGA) (Middle left) en face swept source optical coherence tomography (SS-OCT) image is showing pigment epithelial detachment (Middle right) corresponding B-scan is showing the feeder as hyporeflective line penetrating through the Bruch's membrane (arrowheads) to feed the polyp (crossing yellow lines) (Lower left) flattened en face SS-OCT image is showing diffuse choroidal vascular dilatation at the choroidal vascular layer (Lower right) corresponding flattened B-scan is showing the PED and the feeder vessel (black line represents the C-scan level at the choroidal vascular layer).

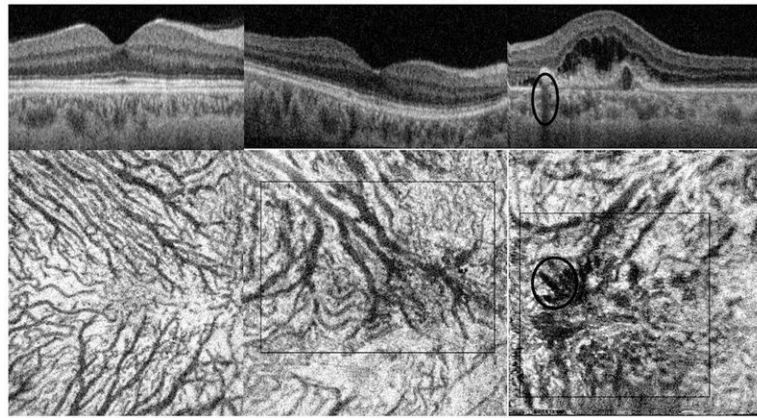


**Figure 7.** Cross-sectional (Top) and en face swept source optical coherence tomography (Bottom) images of (Left) right eye of a 47-year-old Asian normal woman; (Middle) unaffected right eye of a 69-year-old Asian woman with unilateral polypoidal choroidal vasculopathy (PCV); some choroidal vessels are quite large in the center (square) (Right) Affected left eye with PCV; choroidal vascular dilatation is noted (square) and shadow artifacts from the retina exudates are marked with a (oval).



Demographics of patients with polypoidal choroidal vasculopathy and en face swept source optical coherence tomography generated qualitative analysis of the choroidal vasculature.

**Table 1**

Subject	Orientation	Age	VA	Treatment	Location of PED	Choroidal vasculature
1	OD	63	20/30	None	Superior periphery	Branching vascular network above Bruch's membrane
2	OS	69	20/200	None	Juxtafoveal	Focal dilatation
3	OS	61	20/200	None	Peripapillary	Branching vascular network in CV
4	OD		20/70	None	Extrafoveal	Focal dilatation
	OS	74	20/50	None	Juxtafoveal	Branching vascular network in CC
5	OS	71	20/50	Anti-VEGF	Extrafoveal	Diffuse dilatation
6	OD	72	20/30	Anti-VEGF	Subfoveal	Focal dilatation
Fellow Eyes in patients with unilateral PCV						
2	OD	69	20/50	NA	NA	Focal dilatation
5	OD	71	20/50	NA	NA	Diffuse dilatation
6	OS	72	20/20	NA	NA	No abnormalities

OD= right, OS= Left, VA= Visual acuity, PED= Pigment epithelial detachment, Anti-VEGF= Anti-vascular endothelial growth factor, CC= Choriotocapillaris layer, CV= Choroidal vascular layer, NA= Not applicable.

En face swept source optical coherence tomography generated quantitative analysis of the choroid in patients with polypoidal choroidal vasculopathy at the area of the lesion.

**Table 2**

Subject number	Orientation	CC	CV	Total	Location of PED
1	OD	41.3	210.6	251.9	Superior periphery
2	OS	41.3	268.5	309.8	Juxtafoveal
3	OS	45.43	285	330.4	Peripapillary
4	OD	37.2	251.9	289.1	Extrafoveal
	OS	45.4	210.6	256.1	Juxtafoveal
5	OS	41.3	392.4	433.7	Extrafoveal
6	OD	37.2	235.4	272.6	Subfoveal
Average (excluding subject 1)		41.3	274.0	315.3	
Fellow Eyes in patients with unilateral PCV					
2	OD	37.3	243.8	280.8	NA
5	OD	45.4	421.3	466.7	NA
6	OS	45.4	214.8	260.2	NA
Average		42.7	293.2	335.9	
P-value		0.64	0.74	0.73	

CC= choriocapillaris layer, CV= choroidal vascular layer, Total= total choroidal thickness, PED= pigment epithelial detachment, NA= not applicable. P-value represents the significance of the difference between the affected and non-affected eyes in patients with unilateral polypoidal choroidal vasculopathy. Subject 1 with superior peripheral PCV lesion was excluded from the comparison. p-value of < 0.05 was considered statistically significant. All choroidal measurements are in microns (µm).

Summary of the average choroidal thickness (measured at the area of pathology in between the arcades in patients with polypoidal choroidal vasculopathy), and subfoveal choroidal thickness in fellow eyes and normal subjects.

**Table 3**

	N	Age ± SD (years)	CC	CV	Total
PCV eyes	7	68.3 ± 5.2	41.3	274.0	315.3
Fellow eyes	3	70.7 ± 1.5	42.7	293.2	335.9
Normal	10	62.4 ± 12.1	55.8	260.0	315.5
p-value		0.3	0.03*	0.7	0.99

N= number of eyes, CC= choriocapillaris layer, CV= choroidal vascular layer, Total= total choroidal thickness, SD= standard deviation. Fellow eyes are the contralateral non-affected eyes in subjects with unilateral polypoidal choroidal vasculopathy (PCV). All subfoveal choroidal measurements (in between the arcades) are in microns (µm). The subject with the superior peripheral PCV lesion was excluded from the comparison. P-value represents the significance of the difference between eyes with PCV and age-matched normal subjects. p-value of < 0.05 was considered statistically significant.